

Numerical Analysis of the Ricochet of a Conical Nose Projectile in the Collision with Ceramic-Aluminum Armor

Bahman Salimi, Khodadad Vahedi, R.Hosseini, and Masoud Rahmani, Imam Hossein University, Tehran, Iran.

Abstract— The anti-armored bullets have more kinetic energy due to more mass than ordinary bullets, which increases their likelihood of penetration for different target, so it is necessary to seek solutions to reduce the possibility of penetration of these The type of bullets and the increasing likelihood of ricochet them, is one of the ways to increase the likelihood of ricocheting bullets by leveling the surfaces. In this paper, the phenomenon of buckling steel cone with a nose cone in a collision with ceramic targets was investigated by explicit finite element method using LS-Dayna software. in this study the critical angle of ricochet at different speeds. The results of numerical simulation with other empirical results of other researchers have been evaluated that show good accuracy.

Index Terms— Ricochet, simulation, anti-armored bullets, Alumina ceramic.

I. INTRODUCTION

THIS article examines the ricochet of bullets in dealing with aluminum ceramic targets. One of the main phenomena in the design of armored vehicles is the projection ricochet. ricochet of the projectiles means that the projectile is displaced after moving to the angle of the shot and thrown to the other. Considering the importance of this issue in the military industry, many studies have been done in this area. The mechanism of ricochet phenomenon has been examined by the tests of Jonas and Zukas [1]. They concluded that, with increasing collision speeds, tensions increased and, in a particular case, excessive increase in these tensions led to the displacement of the target's hydrodynamics and projectiles near their frontier. Tate [2] presented an analytical model for ricocheting. Gupta [3] studied the effect of the shape of the head of long rod projectiles on normal collisions with the metal thin-walled walls and observed that the ballistic performance of the cone projectiles is better than flat head projectiles. A further analysis of the ricochet phenomenon was presented by Rosenberg. The phenomenon of riding on ceramic surfaces was examined numerically by Wang et al [4]. They concluded that at small angles the projectile hits the direction after the

infiltration in the opposite direction, and tends to be vertical towards the target. But with increasing angle of impact, from certain angles to the next, the projectile turns during the impact and in the direction of the agreement, and as a result, the angle of inclination increases, which is a useful phenomenon to increase the efficiency of armored ceramics. SEIDL and et al [5] explored numerically and experimentally the ricochet projectile in dealing with steel plates. in ceramic because of the brittle structure and the type of impact damage, the penetration resistance is not a constant and can vary depending on the conditions and speed of impact and penetration and even the backing layer conditions. Ricochet of a tungsten heavy alloy long-rod projectile from deformable steel plates Reviewed by Lee [6]. In this paper, a numerical study of the phenomenon of rustling a special type of anti-armored steel projectiles in dealing with alumina ceramic armor with an aluminum support plate of 2024 has been investigated.

II. PROBLEM THEORY

A. Model

In a general overview of the research on abnormal collisions, including non-perturbation collisions, by Goldsmith, the term rhying has been defined as follows: In the event that the projectile does not pierce it after a collision with the target, and does not stand inside the target, it is said to be ricochet. The angle between the projectile path and the normal to target plane is also the angle of inclination, And for any particular speed of the projectile, there is a minimum angle, in which the projectile's angle becomes ricochet. Tate stated that due to the high velocity of the collision and the high speed of the shape and the displacement of the projectile material from the main axis of the projectile, it is possible to directly assume the projectile's penetration. Therefore, the force applied to the front of the projectile tends to produce a capillary in its rigid section. This is the main reason for changing the projectile and ricocheting it.

The end of the projectile is also rigid in its impact on the dynamic resistance of the projectile in the impact phenomenon.

In theory, the effects of the target thickness have not been investigated.

In this theory, the following assumptions are made.

- 1- Slowdown of projectile during infiltration is considered.
- 2- The erosion of the projectile's front surface is equal to the erosion rate in the stable hydrodynamic phase of penetration.
- 3- The effective tension in the end part is considered to be the same as the hydrodynamic resistance of the projectile y_p material.

The optimized equation of the Bernoulli equation by Tate-Alekseevskii [7 and 8] includes equation (1), in this equation, u is the velocity of projectile penetration and R_t is the target's resistance to penetration, ρ_p and ρ_t are the projectile and target density, L and D , the projectile's length and diameter V are the initial velocity of the projectile.

$$\frac{1}{2}\rho_p(v-u)^2 + Y_p = \frac{1}{2}\rho_t U^2 + R_t \quad (1)$$

As a result, the penetration rate is obtained by equation (2).

$$U = \frac{\rho_p v - \sqrt{\rho_p^2 v^2 - (\rho_p - \rho_t)(\rho_p v^2 + 2(Y_p - R_t))}}{\rho_p - \rho_t} \quad (2)$$

For the above relation, according to many experiments, this result is obtained in deep intrusions $R_t = 3Y_p$, assuming that the projectile will be ricochet once the penetration rate is zero, then we will have:

$$V_{crit} = \left[2(R_t - Y_p) / \rho_p \right]^{\frac{1}{2}} \quad (3)$$

At speeds above the supercell, it starts to penetrate the target, but at the same time it redirects.

In Fig.1, the ideal state is a few moments after the projectile has a target with the projectile eroded surface length equal to S , which is calculated as Equation (4).

$$S = (V - U)t / \sin \psi \quad (4)$$

As a result, the vertical force enters the surface is equal to:

$$f = Y_p ds \quad (5)$$

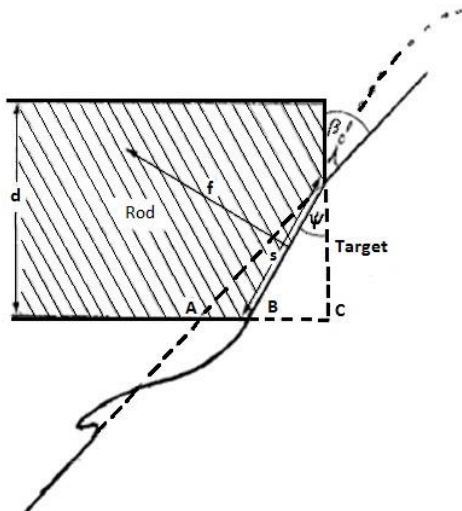


Fig.1. Schematic of projectile- target during t after collision [2]. $AB = U.t$

and $AC = V.t$.

The moment created by this force is calculated around the center of gravity of the projectile, as follows:

$$C = \frac{1}{2} fl \sin \psi \quad (6)$$

Assuming that the projectile does not suffer from a large shape change, and the mean time of its penetration is t_m , the following equation is obtained:

$$t_m = D \tan \beta / V \quad (7)$$

At this time, the coupling C has been given a rotary motion to the projectile, which is shown in the following equation:

$$\ddot{\theta} = \frac{12C}{M(L^2 + D^2)} \quad (8)$$

In the above relation M is the projectile mass and Θ is the angular displacement of the projectile. Ricochet occurs when:

$$\dot{\theta} > 2V \cot \beta / l \quad (9)$$

$$\ddot{\theta} = At$$

$$A = 6Y_p(V - U) / \rho_p D(L^2 + D^2)$$

By the integration of (9), the relation (10) is derived.

$$\dot{\theta} = \frac{1}{2} At^2 \quad (10)$$

Finally, the ricocheting angle is defined as follows.

$$\tan^3 \beta > \frac{2}{3} \frac{\rho_p V^2}{Y_p} \left(\frac{L}{D} + \frac{D}{L} \right) \left(\frac{V}{V - U} \right) \quad (11)$$

The expression (11) at the high collision speeds tends to the following relationship.

$$\tan^3 \beta > \frac{2}{3} \frac{\rho_p V^2}{Y_p} \left(\frac{L^2 + D^2}{LD} \right) \left[1 + \left(\frac{\rho_p}{\rho_t} \right)^{1/2} \right] \quad (12)$$

B. Rosenberg model

In 1989, Rosenberg [9] presented a model for analyzing a ricochet critical angle, which, unlike Tate's theory, was no longer considered rigid. Here, the ricochet is defined as the Tate model.

According to Fig. 1:

$$U = \frac{b}{t} = \frac{x \tan \beta}{t} \quad (13)$$

In this model, contrary to the analytical model of Tate, it is assumed that the amount of force depends on the applied pressure from the target material to the projectile, so, considering R_t , the material resistance will be:

$$f = R_t SD \quad (14)$$

The vertical impact force on the projectile is:

$$I = \int_0^{t_m} f \sin \psi dt = \frac{R_t D^3 (V - U)}{2V^2} \tan \beta \quad (15)$$

$$V_T = \frac{R_t}{\rho_p V^2} \left(\frac{V - U}{V + U} \right) V \cdot \tan \beta \quad (16)$$

Once the projectile is ricochet to have the following condition:

$$\tan \beta > \frac{V}{V_T} \tag{17}$$

Therefore, considering this condition in the above equation, the critical angle of ricocheting in the Rosenberg model is obtained from the following equation:

$$\tan^2 \beta > \frac{\rho_p V^2}{R_t} \left(\frac{V+U}{V-U} \right) \tag{18}$$

The conditions of this model are different in several cases with the Tate model; in Rosenberg's model, the critical angle of riding depends on the target's resistance, while in the Tate model this angle depends on the resistance of the projectile material, this is because the Rosenberg model has a projectile erosion and in the model Tate is considered rigid projectile. As a result, in the Rosenberg theory, due to the unreliability of the projectile, the parameters of projectile length and diameter in the relationship of the critical angle of ricocheting does not appear.

III. RICOCHET ANGLE STUDY WITH NUMERICAL SIMULATION

In this part of the paper, simulation and ricocheting at different speeds ranging from 700 to 1000 m/s are discussed. For this purpose, we will use a steel projectile with a diameter of 7.62 and a length of 25.5 mm made of ceramic material with a backing of aluminum metal. The thickness of the ceramic is 10 mm and the thickness of aluminum is 6 mm. A schematic of the meshed sample is shown in Fig. 2.

The type and characteristics of the support and the projectile and target models for simulating are presented in Table 1.

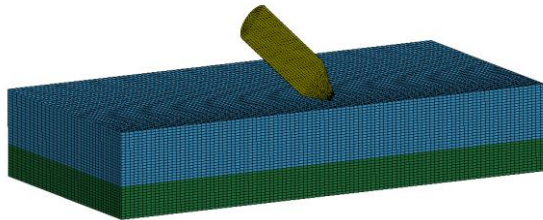


Fig.2. Elemental image of the projectile and the target of simulating the phenomenon of ricochet

TABLE I
BOUNDARY CONDITIONS AND SIMULATIONS MODELS

material	Element type	Material model	Equation of state	boundary conditions
ceramic	Cubic	Johnson <i>holmquist</i>	-	clamp
Steel	Cubic	Johnson Cook	Mie-Gruneisen	free
aluminium	Cubic	Johnson Cook	Mie-Gruneisen	clamp

TABLE II
PROPORTIONAL STEEL MATERIAL MODEL

Amount	Symbol (unit)	Parameter
7800	Ro ($\frac{kg}{m^3}$)	Density
80	G (Gpa)	Shear modulus
210	E (Gpa)	Modulus of elasticity
0.31	PR	Poisson's ratio
507	A (Mpa)	Initial yield strength
320	B (Mpa)	Hardness constant
0.28	C	Strain rate constant
0.15	D_1	First failure parameter
0.72	D_2	Second failure parameter
1.66	D_3	Third failure parameter
0.005	D_4	Fourth failure parameter
-0.84	D_5	Fifth failure parameter
1.70	Γ	Gruneisen parameter

TABLE III
SPECIFICATIONS OF THE 6061 ALUMINUM MATERIAL USED IN SIMULATION

Amount	Symbol (unit)	Parameter
2700	Ro ($\frac{kg}{m^3}$)	Density
26	G (Gpa)	Shear modulus
68	E (Gpa)	Modulus of elasticity
0.33	PR	Poisson's ratio
324	A (Mpa)	Initial yield strength
114	B (Mpa)	Hardness constant
0.002	C	Strain rate constant
-0.77	D_1	First failure parameter
1.45	D_2	Second failure parameter
-0.47	D_3	Third failure parameter
0	D_4	Fourth failure parameter
1.6	D_5	Fifth failure parameter
2.14	Γ	Gruneisen parameter

The specifications for materials used in simulation are presented in Tables 2 through 4.

The specifications of the Al₂O₃ ceramic used in modeling are presented in Table 4.

TABLE IV
SPECIFICATIONS OF THE AL₂O₃ CERAMIC MATERIAL MODEL
USED IN SIMULATION

Amount	Symbol (unit)	Parameter
3800	Ro ($\frac{kg}{m^3}$)	Density
0.989	G (Gpa)	Shear modulus
0.989	A (Gpa)	Normal initial resistance
0.77	B (Gpa)	Normal failure resistance
0	C	Constant strain rate
1	EPSI(s^{-1})	Reference strain rate
0.15	T (Gpa)	Maximum tensile strength
0.5	SFMAX	Maximum Normal failure resistance
5.9	HEL(Gpa)	<i>hugoniot</i> Elastic Limit
2.2	PHEL(Gpa)	Pressure component in <i>hugoniot</i> Elastic Limit
200	(Gpa)K ₁	Bulk modulus
0	(Gpa)K ₂	Second pressure factor
0	(Gpa)K ₃	Third pressure factor
1.5	FS	Failure criterion

IV. RESULTS AND DISCUSSION

One of the main parts of any research work is the validation of the results with other researchers' research. In this section, we use numerical solution validation for comparing the amount of backup layer displacement with experimental values [11]. Fig.3 shows a comparison between the results of the simulation and the experimental results [10] in graphical form.

In the following, it is necessary to consider the critical angle in which the projectile rushes. In Figure 4, you can see that the projectile is at a speed of 1000 m / s at an angle of 30 degrees from the normal line to the surface of the penetration. It is observed in Fig. 5 for an angle of 67 degrees, which makes the projectile after ricochast collisions. In both simulations, the thickness of the ceramic is 10 mm and the aluminum thickness of the back layer is 6 mm.

TABLE V
COMPARISON OF NUMERICAL AND LABORATORY VALUES [11]
FOR THE AMOUNT OF DISPLACEMENT OF THE BACKUP LAYER AT
AN ANGLE OF 0° FROM THE NORMAL LINE ON THE SURFACE

Test number	Collision speed(m/s)	Numerical results (mm)	Exprentage results (mm)	Percentage error
1	775	14.67	14.91	1.61
2	844	16.35	17.77	7.99
3	378	8.58	7.62	12.60
4	266	6.41	7.33	12.55
5	287	6.57	6.11	7.53

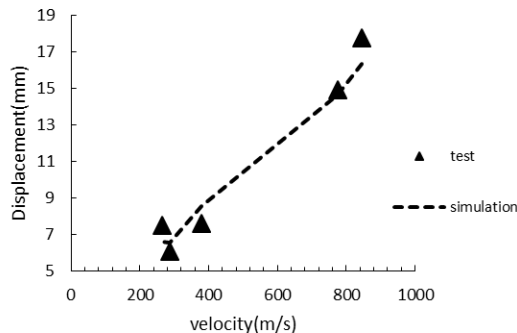


Fig.3. Comparison between simulation results and laboratory results [11]

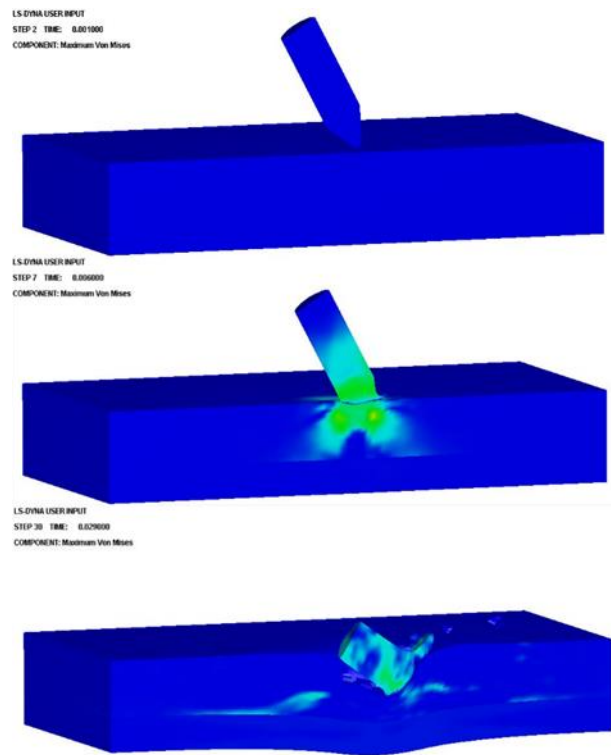


Fig.4. The projectile penetrates at 1000 m / s and 30 degrees to the normal line on the surface

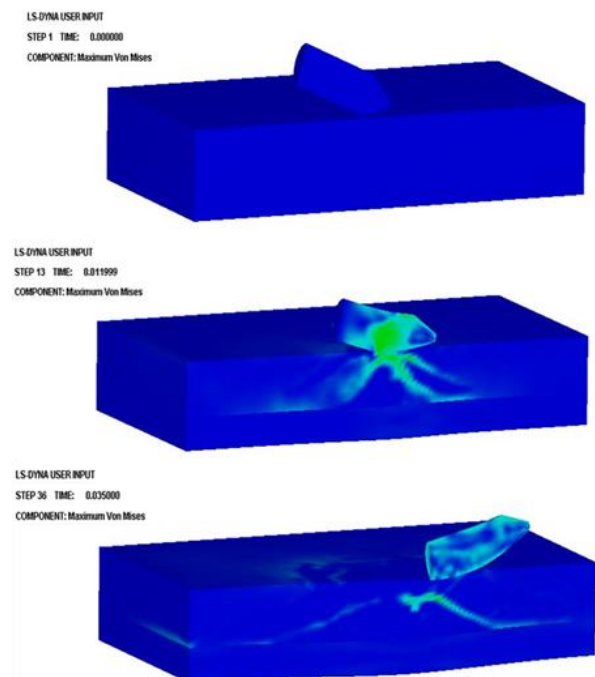


Fig.5. Ricocheting the projectiles at a speed of 1000 m / s and an angle of 67 degrees from the normal line on the surface

In Figures 6 and 7, variations in the projectile velocity at collision angles of 30 and 67 degrees are given. It can be seen that the critical angle can also be calculated using the analytical relationship extracted in Section III.

It should be noted that when the projectile hits the surface, the projectile is eroded, and the projectile mass also changes with time, and the projectile erosion also depends on the angle of impact, the projectile's speed, and other parameters. In Figs. 8 and 9, the kinetic energy changes observed by simulation are visible.

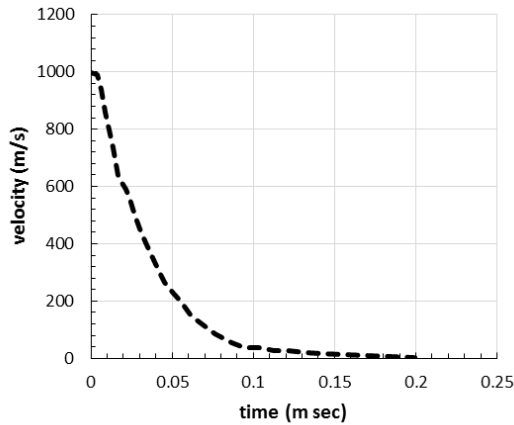


Fig.6. The variation of the projectile's velocity at penetration angles of 30 degrees compared to the normal line

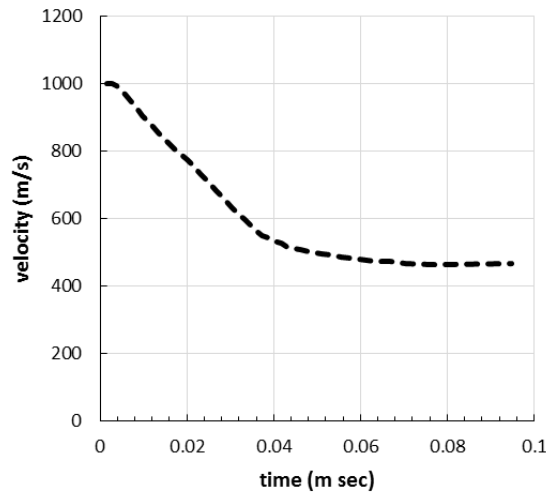


Fig.7. The variations in the projectile's velocity at a steady angle of 67 ° from the normal line

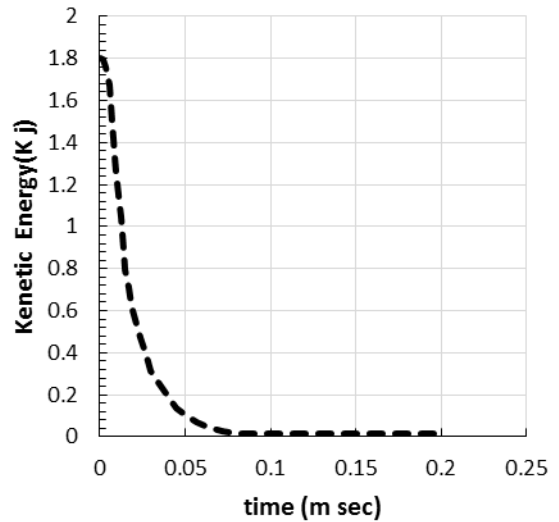


Fig.8. The kinetic energy changes of the projectile with an angle of 30 degrees relative to the normal line (the projectile penetrates)

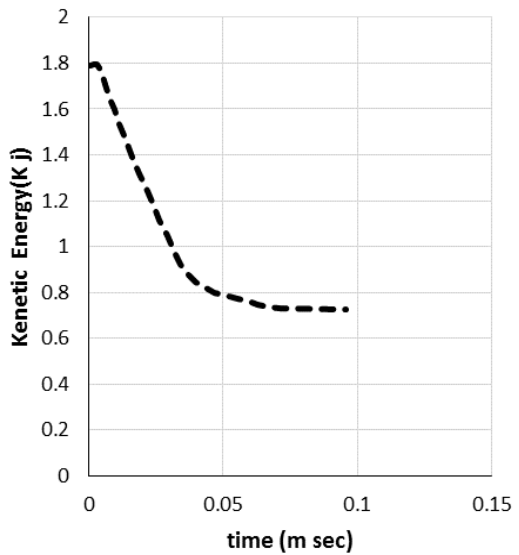


Fig.9. The kinetic energy changes of the projectile with a collision angle of 67 degrees relative to the normal line (ricochet projectile)

I. CONCLUSION

In this paper, we investigated the explicit numerical solving of the rusting of anti-armored steel projectiles in dealing with alumina ceramic armor with an aluminum support plate. It was observed that the simulation results are in good agreement with experimental work. With regard to the simulation and analytical relationships, it is clear that with increasing speed the angle of the buckling angle is increased and the probability of penetration of the projectile is higher.

REFERENCES

- [1] G. Jonas and J. A. Zukas, "Mechanics of penetration: analysis and experiment," *International Journal of Engineering Science*, vol. 16, pp. 879-903, 1978.
- [2] A. Tate, "A simple estimate of the minimum target obliquity required for the ricochet of a high speed long rod projectile," *Journal of physics. D. Applied physics*, vol. 12, pp. 1825-1829, 1979.
- [3] N. Gupta, M. Iqbal, and G. Sekhon, "Experimental and numerical studies on the behavior of thin aluminum plates subjected to impact by blunt-and hemispherical-nosed projectiles," *International Journal of Impact Engineering*, vol. 32, pp. 1921-1944, 2006.
- [4] Z. Q. Wang, X. J. Tang, X. T. Wang, X. N. Meng, and H. Q. Lv, "Numerical simulation on the oblique penetration of ceramic particles reinforced metal matrix functional gradient armor," in *Key Engineering Materials*, 2014, pp. 585-588.
- [5] SEIDL, MARINA, THOMAS WOLF, and RAINER NUESING. "Numerical Investigations on Ricochet of a Spinstabilised Projectile on Differently Shaped Target Surfaces." 30th International Symposium on Ballistics. 2017.
- [6] W. Lee, H.-J. Lee, and H. Shin, "Ricochet of a tungsten heavy alloy long-rod projectile from deformable steel plates," *Journal of Physics D: Applied Physics*, vol. 35, p. 2676, 2002.
- [7] V. Alekseevskii, "Penetration of a rod into a target at high velocity," *Combustion, Explosion, and Shock Waves*, vol. 2, pp. 63-66, 1966.
- [8] A. Tate, "A theory for the deceleration of long rods after impact," *Journal of the Mechanics and Physics of Solids*, vol. 15, pp. 387-399, 1967.
- [9] Z. Rosenberg, Y. Yeshurun, and M. Mayseless, "On the ricochet of long rod projectiles," in *Proc. 11th Int. Symp. Ballistics*, 1989.
- [10] G. R. Johnson and W. H. Cook, "Fracture characteristics of three metals subjected to various strains, strain rates, temperatures and pressures," *Engineering fracture mechanics*, vol. 21, pp. 31-48, 1985.
- [11] Alizadeh, Vahedi Khodadad, "Analytical and Numerical Investigation of Penetration of Conical Projectiles into FML Targets", *Quarterly Journal of Aerospace Mechanics*, vol. 10th of April 2014 (in Persian).